

TTP04-20  
SI-HEP-2004-09

# Modeling the Pion and Kaon Form Factors in the Timelike Region

**Christine Bruch <sup>a)</sup>, Alexander Khodjamirian <sup>b)</sup>,  
Johann H. Kühn <sup>a)</sup>**

<sup>a)</sup>*Institut für Theoretische Teilchenphysik, Universität Karlsruhe,  
D-76128 Karlsruhe, Germany*

<sup>b)</sup> *Theoretische Physik 1, Fachbereich Physik, Universität Siegen,  
D-57068 Siegen, Germany*

## Abstract

New, accurate measurements of the pion and kaon electromagnetic form factors are expected in the near future from experiments at electron-positron colliders, using the radiative return method. We construct a model for the timelike pion electromagnetic form factor, that is valid also at momentum transfers far above the  $\rho$  resonance. The ansatz is based on vector dominance and includes a pattern of radial excitations expected from dual resonance models. The form factor is fitted to the existing data in the timelike region, continued to the spacelike region and compared with the measurements there and with the QCD predictions. Furthermore, the model is extended to the kaon electromagnetic form factor. Using isospin and SU(3)-flavour symmetry relations we extract the isospin-one contribution and predict the kaon weak form factor accessible in semileptonic  $\tau$  decays.

# 1 Introduction

The pion electromagnetic (e.m.) form factor  $F_\pi(s)$ , one of the traditional study objects in hadron physics, nowadays plays an essential role for the precise determination of electroweak observables. An accurate knowledge of  $F_\pi(s)$  at timelike momentum transfers  $s > 4m_\pi^2$  is needed to calculate the hadronic loop contribution to the muon anomalous magnetic moment and to the running of the e.m. coupling (see [1, 2] for the current status).

New accurate data on the pion form factor in the timelike region have recently been obtained by the CMD-2 collaboration [3] measuring the  $e^+e^- \rightarrow \pi^+\pi^-$  cross section at  $\sqrt{s} = 0.61 \div 0.96$  GeV (for an update of these data see [4]). In this region, it is successfully described (fitted) using models based on  $\rho$ -meson dominance, with a small but clearly visible  $\omega$ -meson admixture. Above 1 GeV data on  $e^+e^- \rightarrow \pi^+\pi^-$  [5, 6, 7] exist but are not that accurate. Employing isospin symmetry one also gains independent information from the measurements of  $\tau \rightarrow \pi^-\pi^0\nu_\tau$  at  $s < m_\tau^2$  (for details see, e.g. [1]). There are other interesting form factors closely related to  $F_\pi$ : the charged (neutral) kaon e.m. form factors measured in  $e^+e^- \rightarrow K^+K^-$  ( $e^+e^- \rightarrow K^0\bar{K}^0$ ), as well as the weak transition form factor accessible in  $\tau \rightarrow K^-K^0\nu_\tau$ .

In the near future the experimental knowledge on  $F_{\pi,K}(s)$  will be substantially improved, due to new data to be obtained using the radiative return method [8]. The first measurements of  $F_\pi$  with this technique in the  $\rho$  region have already been performed by the KLOE Collaboration [9] and the agreement with the CMD-2 data is encouraging. At larger energies, up to 2.0-2.5 GeV, perhaps even 3 GeV, accurate measurements of  $F_{\pi,K}$  are anticipated from the BABAR experiment (for preliminary results see [10]). The high rates expected at  $s \gg m_\rho^2$  demand phenomenological models more elaborated than the simple  $\rho$ - ( $\rho, \omega, \phi$ -) dominance models for  $F_\pi$  ( $F_K$ ). The main purpose of this paper is to construct an ansatz for the pion form factor that is valid in the region below and far above  $\rho$ -resonance and to extend this model to the kaon form factor.

The model is constructed to obey the constraints from analyticity and isospin-symmetry and to incorporate the proper behaviour at high energies, consistent with perturbative QCD, and the correct normalization at  $s = 0$ . Furthermore it is based on plausible assumptions derived from the quark model, moderate SU(3)-breaking, vector dominance and a pattern of radial excitations expected from dual resonance models. It has enough flexibility to accommodate the characteristic interference pattern of the cross section and, once sufficiently precise data are available at higher energies, may be used to fix the parameters of the higher excitations.

Above the  $\rho$ -resonance the excited  $\rho'(1450)$  and  $\rho''(1700)$  are expected to play an important role. Already now these two states are indispensable, if one wants to accommodate the measured parameters of the  $\rho$ -resonance with the correct normalization of  $F_\pi(s)$  at  $s = 0$ , as demonstrated by earlier analyses and fits within the  $\rho$  region (see, e.g. [11, 12]). In general, to include all possible intermediate hadronic states in the  $\gamma^* \rightarrow \pi^+\pi^-$  transition amplitude, one has to take into account an infinite series of radially excited  $\rho$ 's. In addition, there are multihadron intermediate states with  $J^P = 1^-$  and  $I = 1$  ( $2\pi, 4\pi, K\bar{K}$

etc.). Hence, the pion form factor at timelike  $s > m_\rho^2$  is a complicated object determined by a large or even infinite amount of hadronic parameters not accessible at present in a rigorous theoretical framework.

On the other hand, at sufficiently large  $s$  one expects  $F_\pi(s) \sim \alpha_s(s)/s$ , as predicted from perturbative QCD [13] for the pion form factor in the spacelike region at  $s \rightarrow -\infty$ , analytically continued to  $s \rightarrow +\infty$ . In other words, the overlap of many intermediate hadronic states has to build up a smooth, power-behaved function. One might consider using this QCD prediction in the region of present interest, that is, at intermediate timelike  $s$ . However, data on the form factor in the spacelike region,  $s < 0$ , indicate that the onset of this asymptotic behaviour is far from the “few  $\text{GeV}^2$ ” region. Preasymptotic contributions  $\sim 1/s^n$  with  $n > 1$ , stemming from the end-point, soft mechanism [14] are essential for  $s \sim 1 - 10 \text{ GeV}^2$ . Approximate methods valid at intermediate spacelike momenta, for example QCD sum rules [15, 16, 17], allow to calculate  $F_\pi(s)$  including soft effects. However, a straightforward analytic continuation of  $F_\pi(s < 0)$  to large  $s > 0$  is difficult. The timelike form factor will suffer from uncertainties in the analytic continuation of soft parts, Sudakov logs and of  $\alpha_s(s)$  (for a discussion see [18, 19]). Hence, QCD calculations cannot be directly used in the large  $s > 0$  region, e.g., for estimating the “tail” of higher resonances in the form factor. In this paper we therefore prefer to adopt a model for the pion form-factor formulated entirely in terms of hadronic degrees of freedom. Importantly, the form factor, as obtained from the model, fitted in the time-like region and extrapolated to spacelike momenta, has a proper power-law behaviour which can be compared with the data at  $s < 0$  and used to test various QCD-based predictions.

Models of hadronic amplitudes, where an infinite series of resonances at  $s > 0$  is summed to yield a power-law behaviour at  $s < 0$ , are rooted in the Veneziano amplitude and dual resonance models formulated long before the advent of QCD. Importantly, the pattern of infinite zero-width resonances is predicted in the  $N_c = \infty$  limit of QCD. Recently, the model for the pion form factor using the masses and coefficients chosen according to Veneziano amplitude was considered in [20]. Earlier, similar analyses of the pion form factor can be found in [21]. Models of dual-resonance type with infinite number of resonances are widely used also for other hadronic problems, some recent works can be found in [22]. We will use the dual-QCD $_{N_c=\infty}$  model [20] as a starting point, modifying it for the first few  $\rho$  resonances, by keeping their parameters (masses, widths and coefficients) free and fitting them to experiment. In this way, the complicated effects of  $\rho$  resonances coupled to multihadron ( $2\pi, 4\pi$  etc.) states are implicitly taken into account. It is remarkable that the gross features of the model are well reproduced with the (fitted) resonance parameters. Since in the dual-resonance amplitude the coefficients of higher resonance contributions decrease with the resonance number, the corresponding modifications for individual higher states are not important, and the “tail” of resonances is treated as in [20]. The model for the pion form factor is also analytically continued to the spacelike region and compared with the data there and with the QCD predictions on  $F_\pi(s)$  at large spacelike  $s$ .

Furthermore, we extend the model to the kaon form factor, employing an SU(3)-generalization of the pion amplitude. Fitting the charged and neutral kaon form factors to the data, and using flavour symmetries, we predict the weak kaon form factor relevant

for  $\tau$  semileptonic decays. Let us also mention at this point that the decomposition of the form factors into their isospin zero and one components respectively, is also of relevance for a model-independent evaluation of  $\gamma$ -Z-mixing [23] where the two amplitudes contribute with a different relative weight.

The plan of the paper is as follows. In Section 2 we summarize the phenomenology of  $F_\pi(s)$  recalling the derivation of the  $\rho$ -meson contribution, whereas in Section 3 the contributions of excited  $\rho$  resonances are discussed. The model for the pion form factor is introduced in Section 4 and its parameters are fitted to the data. In Section 5 we proceed to the kaon e.m. form factors and Section 6 is devoted to the weak kaon form factor in  $\tau$  decays. Section 7 contains our summary and conclusions.

## 2 The $\rho$ -meson contribution to the pion form factor

The pion e.m. form factor is defined in the standard way,

$$\langle \pi^+(p_1) \pi^-(p_2) | j_\mu^{em} | 0 \rangle = (p_1 - p_2)_\mu F_\pi(s) \quad (1)$$

The quark e.m. current  $j_\mu^{em} = \sum_{q=u,d,s} e_q \bar{q} \gamma_\mu q$  can be decomposed into isospin one and zero components respectively. At the quark level this corresponds to

$$j_\mu^{em} = \frac{1}{\sqrt{2}} j_\mu^3 + \frac{1}{3\sqrt{2}} j_\mu^{I=0} - \frac{1}{3} j_\mu^s \quad (2)$$

with

$$j_\mu^3 = (\bar{u} \gamma_\mu u - \bar{d} \gamma_\mu d) / \sqrt{2}, \quad j_\mu^{I=0} = (\bar{u} \gamma_\mu u + \bar{d} \gamma_\mu d) / \sqrt{2}, \quad j_\mu^s = \bar{s} \gamma_\mu s. \quad (3)$$

The isotriplet partners of the current  $j_\mu^3$  form the charged weak current

$$j_\mu^- = (j_\mu^1 + i j_\mu^2) / \sqrt{2} = \bar{u} \gamma_\mu d. \quad (4)$$

In the isospin symmetry limit, the  $I = 0$  and  $s$ -quark components of the current do not contribute to  $F_\pi$ . In Eq. (1),  $s = (p_1 + p_2)^2$  is the timelike momentum transfer squared,  $s \geq 4m_\pi^2$ . The form factor  $F_\pi(s)$ , being analytically continued to the spacelike region  $s < 0$ , corresponds to the hadronic matrix element  $\langle \pi^+(p_1) | j_\mu^{em} | \pi^+(-p_2) \rangle$  related to Eq. (1) by crossing-symmetry.

There are very few model-independent relations determining or constraining the pion form factor. One of them is the normalization condition for the pion electric charge,

$$F_\pi(0) = 1. \quad (5)$$

An important role is played by the dispersion relation,

$$F_\pi(s) = \frac{1}{\pi} \int_{4m_\pi^2}^{\infty} ds \frac{\text{Im} F_\pi(s')}{s' - s - i\epsilon}. \quad (6)$$

The asymptotic behaviour expected from perturbative QCD [13],

$$\lim_{s \rightarrow -\infty} F_\pi(s) \sim \frac{\alpha_s}{s}, \quad (7)$$

allows for an unsubtracted dispersion relation. The application of Eq. (6) is based on an independent equation for the imaginary part of the form factor derived from the unitarity condition,

$$2\text{Im}F_\pi(s)(p_1 - p_2)_\mu = \sum_h \int d\tau_h \langle \pi^+(p_1)\pi^-(p_2) | h \rangle \langle h | j_\mu^{em} | 0 \rangle^*, \quad (8)$$

where all possible hadronic states  $h$  with  $J^{PC}(I^G) = 1^{--}(1^+)$  are inserted. Each term in the sum in Eq. (8) includes the integration over the phase space and the summation over polarizations of the intermediate state  $h$ . Since isospin symmetry is not exact, there could also be a small admixture of the isospin-zero  $J^{PC} = 1^{--}$  states, e.g. the  $\omega$  and its radial excitations.

Experimental data reveal that at low  $s \leq 1 \text{ GeV}^2$  the most important contribution to Eq. (8) stems from  $\rho$  meson. The  $\rho$ -meson decay constant:

$$\langle \rho^0 | j_\mu^{em} | 0 \rangle = \frac{m_\rho f_\rho}{\sqrt{2}} \epsilon_\mu^{(\rho)*}, \quad (9)$$

and the strong  $\rho\pi\pi$  coupling:

$$\langle \pi^+(p_1)\pi^-(p_2) | \rho^0 \rangle = (p_2 - p_1)^\alpha \epsilon_\alpha^{(\rho)} g_{\rho\pi\pi}, \quad (10)$$

(where  $\epsilon^{(\rho)}$  is the  $\rho$ -meson polarization four-vector) determine the  $\rho$ -contribution to the imaginary part of the pion form factor in the narrow width approximation:

$$\text{Im}F_\pi^{(\rho)}(s) = \frac{m_\rho f_\rho}{\sqrt{2}} g_{\rho\pi\pi} \pi \delta(s - m_\rho^2). \quad (11)$$

Substituting this into the dispersion relation (6) gives:

$$F_\pi^{(\rho)}(s) = \frac{m_\rho f_\rho g_{\rho\pi\pi}}{\sqrt{2}(m_\rho^2 - s - i\epsilon)}. \quad (12)$$

The excited  $\rho', \dots$  resonances have contributions of the same form, with the decay constants  $f_{\rho', \dots}$  and strong couplings  $g_{\rho'\pi\pi}, \dots$

The pion form factor constructed by adding up the zero-width  $\rho, \rho', \dots$  -resonances is an oversimplified ansatz which cannot be used at  $s > 0$  where the experimentally observable large widths of these resonances are important. The widths are generated by the contributions of multi-hadron states to the imaginary part of  $F_\pi$ , starting from the lowest two-pion state. The contribution of the latter to the unitarity relation

$$2\text{Im}F_\pi^{(2\pi)}(s)(p_1 - p_2)_\mu = \int d\tau_{2\pi} (p'_1 - p'_2)_\mu A_{\pi\pi}(s) F_\pi^*(s), \quad (13)$$

involves the two-pion phase space :

$$d\tau_{2\pi} = \frac{d^3 p'_1}{(2\pi)^3 2E'_1} \frac{d^3 p'_2}{(2\pi)^3 2E'_2} (2\pi)^4 \delta^4(p'_1 + p'_2 - p_1 - p_2)$$

where  $(p'_1 + p'_2)^2 = s$  and  $A_{\pi\pi}(s)$  is the amplitude of the strong pion-pion P-wave elastic scattering:

$$A_{\pi\pi}(s) = \langle \pi^+(p_1) \pi^-(p_2) | \pi^+(p'_1) \pi^-(p'_2) \rangle_{I=1, J=1}. \quad (14)$$

In the low-energy region  $4m_\pi^2 < s < 16m_\pi^2$ , the two-pion state is the only contribution to the unitarity relation <sup>1</sup>. At larger  $s$ , vector mesons and various multihadron states contribute, making a model-independent use of Eq. (8) impossible.

A well-known and experimentally supported approach which we adopt here is “vector dominance”. In its simplest form it assumes that the  $\rho$  resonance saturates the pion form factor (Eq. (12)), thus requiring  $f_\rho g_{\rho\pi\pi}/\sqrt{2}m_\rho = 1$ . One furthermore approximates the pion-pion scattering amplitude with an intermediate  $\rho$  exchange. Inserting the intermediate  $\rho$  propagator in Eq. (14) and using the definition (10) we obtain:

$$A_{\pi\pi}(s) \simeq \frac{\langle \pi^+(p_1) \pi^-(p_2) | \rho^0 \rangle \langle \rho^0 | \pi^+(p'_1) \pi^-(p'_2) \rangle}{m_\rho^2 - s} = -\frac{g_{\rho\pi\pi}^2 (p_2 - p_1) \cdot (p'_2 - p'_1)}{(m_\rho^2 - s)}. \quad (15)$$

Substituting this ansatz together with Eq. (12) in Eq. (13), and integrating out the two-pion phase space with the help of

$$\int d\tau_{2\pi} (p'_2 - p'_1)_\alpha (p'_1 - p'_2)_\mu = \left( g_{\alpha\mu} - \frac{(p_1 + p_2)_\alpha (p_1 + p_2)_\mu}{s} \right) \frac{[p(s)]^3}{3\pi\sqrt{s}}, \quad (16)$$

where  $p(s) = \frac{1}{2}(s - 4m_\pi^2)^{1/2}$  is the pion momentum in c.m. frame of two pions, we finally transform Eq. (13) to

$$\text{Im}F_\pi^{(2\pi)}(s) = \frac{m_\rho f_\rho}{\sqrt{2}(m_\rho^2 - s)} \left\{ \frac{g_{\rho\pi\pi}^2 [p(s)]^3}{6\pi\sqrt{s}} \right\} \frac{g_{\rho\pi\pi}}{m_\rho^2 - s}. \quad (17)$$

This formula justifies using the more general expression

$$F_\pi^{(2\pi)}(s) = \frac{m_\rho f_\rho}{\sqrt{2}(m_\rho^2 - s)} \mathcal{A}^{(2\pi)}(s) \frac{g_{\rho\pi\pi}}{m_\rho^2 - s}, \quad (18)$$

which can be interpreted as a two-pion loop insertion in the  $\rho$  meson propagator. The amplitude  $\mathcal{A}^{(2\pi)}(s)$  has a real and imaginary part. A natural approximation for  $\text{Im}\mathcal{A}^{(2\pi)}$  is the expression in curly brackets in Eq. (17). At  $s = m_\rho^2$  it is normalized to the  $\rho \rightarrow 2\pi$  width

$$\text{Im}\mathcal{A}^{(2\pi)}(m_\rho^2) = m_\rho \Gamma(\rho \rightarrow 2\pi) = \frac{g_{\rho\pi\pi}^2}{6\pi m_\rho} [p(m_\rho^2)]^3, \quad (19)$$

---

<sup>1</sup>For a review on the low-energy pion form factor see [24].

To account for all possible amplitudes with two-pion insertions in the  $\rho$ -meson propagator, Eq. (18) has to be added to Eq. (12), together with subsequent diagrams with two, three, etc. two-pion loops. Summing up this geometrical series yields:

$$F_\pi^{(\rho+2\pi)}(s) = \left( \frac{f_\rho g_{\rho\pi\pi}}{\sqrt{2}m_\rho} \right) \frac{m_\rho^2}{m_\rho^2 - s - \text{Re}\mathcal{A}^{(2\pi)}(s) - i\text{Im}\mathcal{A}^{(2\pi)}(s)}, \quad (20)$$

for the part of  $F_\pi$  which contains, in addition to the  $\rho$ -meson, the contributions of the 2-pion intermediate state coupled to  $\rho$ .

Several options for Eq. (20) are in usage. The simplest one is to neglect the real part of  $\mathcal{A}^{(2\pi)}(s)$  and to approximate the imaginary part by a constant, given by Eq. (19). This gives the usual Breit-Wigner (BW) formula for the  $\rho$  resonance with a constant width. A more refined version (used e.g. in [12]) takes into account the  $s$ -dependence of  $\text{Im}\mathcal{A}^{(2\pi)}(s)$  in the form of the  $p$ -wave two-pion phase space (as indicated by Eq. (17)) with the normalization from Eq. (19):

$$\text{Re}\mathcal{A}^{(2\pi)}(s) = 0, \quad \text{Im}\mathcal{A}^{(2\pi)}(s) = \sqrt{s} \frac{m_\rho^2}{s} \left( \frac{p(s)}{p(m_\rho^2)} \right)^3 \Gamma(\rho \rightarrow 2\pi) \equiv \sqrt{s} \Gamma_{\rho \rightarrow 2\pi}(s). \quad (21)$$

The function  $\Gamma_{\rho \rightarrow 2\pi}(s)$  naturally vanishes at  $s < 4m_\pi^2$ , below the  $2\pi$  threshold.

The Gounaris-Sakurai (GS) approach [25] represents another option widely used. In this case one takes into account a nonvanishing real part of  $\mathcal{A}^{(2\pi)}(s)$  calculated from the dispersion relation with two subtractions at  $s = 0$ :

$$\mathcal{A}^{(2\pi)}(s) = \mathcal{A}^{(2\pi)}(0) + s \frac{d\mathcal{A}^{(2\pi)}(0)}{ds} + \frac{s^2}{\pi} \int_{4m_\pi^2}^{\infty} ds' \frac{\text{Im}\mathcal{A}^{(2\pi)}(s')}{s'^2(s' - s - i\epsilon)}. \quad (22)$$

Using the expression for the imaginary part given in Eq. (21) and changing the integration variable from  $s'$  to  $v' = \sqrt{1 - 4m_\pi^2/s'}$  one transforms the integral in Eq. (22):

$$\begin{aligned} s^2 \int_{4m_\pi^2}^{\infty} ds' \frac{\text{Im}\mathcal{A}^{(2\pi)}(s')}{s'^2(s' - s - i\epsilon)} &= \left( \frac{m_\rho^2 \Gamma(\rho \rightarrow 2\pi)}{8[p(m_\rho)]^3} \right) I(s), \\ I(s) &= \frac{s}{v} \int_0^1 dv' v'^4 \left[ \frac{1}{v' - v - i\epsilon} - \frac{1}{v' + v} \right]. \end{aligned} \quad (23)$$

Calculating the principal value of the integral yields the real part:

$$\text{Re}I(s) = s \left( \frac{2}{3} + 2v^2 - v^3 \log \frac{1+v}{1-v} \right). \quad (24)$$

Using the above result in Eq. (22) one obtains the real part of the amplitude  $\mathcal{A}^{(2\pi)}$ . Furthermore, following [25] the subtraction terms are fixed by the normalization conditions

for the mass and the width of the  $\rho$ :  $\text{Re}\mathcal{A}^{(2\pi)}(m_\rho^2) = 0$  and  $\frac{d}{ds}\text{Re}\mathcal{A}^{(2\pi)}(m_\rho^2) = 0$ . At  $s = 0$  the form factor is normalized to unity. Hence

$$F_\pi^{(\rho+2\pi)}(s) = \left( \frac{f_\rho g_{\rho\pi\pi}}{\sqrt{2}m_\rho} \right) \frac{m_\rho^2 + H(0)}{m_\rho^2 - s + H(s) - i\sqrt{s}\Gamma_{\rho\rightarrow 2\pi}(s)}, \quad (25)$$

where we use the same notation as in [12]:

$$H(s) = \hat{H}(s) - \hat{H}(m_\rho^2) - (s - m_\rho^2) \frac{d}{ds} \hat{H}(m_\rho^2), \quad (26)$$

so that

$$\hat{H}(s) = \left( \frac{m_\rho^2 \Gamma(\rho \rightarrow 2\pi)}{2\pi[p(m_\rho)]^3} \right) \left( \frac{s}{4} - m_\pi^2 \right) v \log \frac{1+v}{1-v}. \quad (27)$$

From experiment  $\Gamma(\rho \rightarrow 2\pi) \simeq \Gamma_{tot}(\rho)$ , hence the couplings of  $\rho$  to other intermediate states can be safely be neglected. Therefore we replace in both versions of the BW formula the  $\rho \rightarrow 2\pi$  width by the total width removing the superscript  $2\pi$  at the form factor.

Finally, the  $\rho$  contribution to the pion form factor introduced in Eq. (12) in the zero-width approximation and modified to include the width in Eq. (20), can be rewritten in the following generic form:

$$F_\pi^{(\rho)}(s) = c_\rho BW_\rho(s) \quad (28)$$

where  $c_\rho \equiv F_\pi^{(\rho)}(0)$  is the normalization coefficient. In the adopted approximation is determined by the product of  $\rho$  decay constants and  $\rho\pi\pi$  coupling:

$$c_\rho = \frac{f_\rho g_{\rho\pi\pi}}{\sqrt{2}m_\rho}, \quad (29)$$

and  $BW_\rho(s)$  is the BW formula normalized to unity at  $s = 0$ . For this formula two different versions will be used, one taken from [12]:

$$BW_\rho^{KS}(s) = \frac{m_\rho^2}{m_\rho^2 - s - i\sqrt{s}\Gamma_\rho(s)}, \quad (30)$$

and the one from [25]

$$BW_\rho^{GS}(s) = \frac{m_\rho^2 + H(0)}{m_\rho^2 - s + H(s) - i\sqrt{s}\Gamma_\rho(s)}. \quad (31)$$

In both cases the effective  $s$ -dependent width is assumed to be

$$\Gamma_\rho(s) = \Gamma_{\rho\rightarrow 2\pi}(s), \quad (32)$$

with r.h.s. defined in Eq. (21) and  $\Gamma_\rho(m_\rho^2) = \Gamma_\rho^{tot}$ .

### 3 Contributions of excited $\rho$ states

As already realized in earlier analyses of the pion form factor (e.g., in [11, 12]), the single  $\rho$ -meson approximation is not sufficient to fulfil the normalization condition (5). Indeed, taking the measured values for  $\Gamma(\rho \rightarrow l^+l^-)$  and  $\Gamma(\rho \rightarrow 2\pi)$  from [26] we obtain  $f_\rho = 220$  MeV and, respectively  $g_{\rho\pi\pi} = 6.0$ , yielding  $c_\rho \simeq 1.2$ . One needs to include the contributions of excited  $\rho$  resonances to restore the correct normalization. Currently, two of them,  $\rho'(1450)$  and  $\rho''(1700)$ , are well established experimentally [26]. Adding the contributions of these two states in the form (28) to  $F_\pi^{(\rho)}$ , one fits experimental data on  $e^+e^- \rightarrow 2\pi$  in the  $\rho$ -region, practically up to  $s = 1$  GeV, restoring the normalization condition  $F_\pi(0) = 1$ . Both models (30) and (31) work well. In addition, there is a small isospin-violating effect from  $\omega$  noticeable in the vicinity of  $\rho$ . In what follows, it will be taken into account as in [12], by adding a  $\rho - \omega$  mixing term to the  $\rho$  contribution:

$$F_\pi^{(\rho)}(s) \rightarrow \frac{c_\rho BW_\rho(s)}{1 + c_\omega} (1 + c_\omega BW_\omega). \quad (33)$$

Note, however, that the dominant decays of excited  $\rho$ 's are to final states other than  $2\pi$ , hence the couplings of these resonances to various multiparticle intermediate states ( $4\pi$ ,  $K\bar{K}$  etc.) become important at larger  $s$ , the region of our interest. In the previous section we have seen that the coupling of  $\rho$  to the  $2\pi$  state results in a geometrical series of  $2\pi$ -insertions into the  $\rho$  propagator yielding an imaginary part normalized to the  $\rho \rightarrow 2\pi$  width in the formula for  $BW_\rho$ . The analogous summation procedure can be repeated for each multihadron state coupled to a given excited  $\rho$ , say, to  $\rho'(1450)$ . This leads to a formula for the  $\rho'$  contribution to  $F_\pi$  similar to Eq. (28), where  $\rho \rightarrow \rho'$  and the effective width in  $BW_{\rho'}(s)$  is a sum over the effective widths for each channel

$$\Gamma_{\rho'}(s) = \Gamma_{\rho' \rightarrow 2\pi}(s) + \Gamma_{\rho' \rightarrow 4\pi}(s) + \Gamma_{\rho' \rightarrow 2\pi}(s) + \Gamma_{\rho' \rightarrow K\bar{K}}(s) + \dots \quad (34)$$

All we know about the functions on r.h.s. is their normalization at  $s = m_{\rho'}^2$  to the corresponding partial width of  $\rho'$ , so that altogether  $\Gamma_{\rho'}(m_{\rho'}^2) = \Gamma_{\rho'}^{tot}$ . The  $s$ -dependence for each partial width has to be introduced in a model-dependent way, requiring detailed information on  $4\pi$  (see e.g., [27]) and other hadronic final states in  $e^+e^-$ . In particular, to account for a proper threshold behaviour one has to introduce phase space factors for each  $\Gamma_{\rho' \rightarrow f}$  in Eq. (34), different from the  $p$ -wave factor for  $\Gamma_\rho(s)$ . A complete kinematical and dynamical analysis of the partial widths for excited  $\rho$  resonances is beyond our task (some models can be found in [28]). We will continue using the same ansatz as for  $\rho$ , with the simple  $p$ -wave threshold factor, having in mind that there is still a room for improvement at this point. We have checked that small modifications of the effective width, e.g., replacing the effective threshold by  $4m_\pi$  have little influence on the form factor.

Furthermore, the couplings of different vector resonances to one and the same multihadron state generate mixing between these resonances. To give an example of this effect return to the unitarity relation (13) and substitute on r.h.s. the  $\rho'$  resonance contribution to the form factor while keeping the intermediate  $\rho$  exchange for  $A_{\pi\pi}$ . This term corresponds to a chain of transitions  $\gamma^* \rightarrow \rho' \rightarrow 2\pi \rightarrow \rho \rightarrow 2\pi$ . This nondiagonal amplitude

is clearly not accounted for by the  $2\pi$  insertions to the individual  $\rho$ - and  $\rho'$ -propagators. One has to add to the form factor new terms with the products of two BW propagators, e.g. the  $\rho'$  contribution to the form factor will have the following schematic form:

$$F_\pi^{(\rho')}(s) = c_{\rho'} BW_{\rho'}(s)(1 + x_{\rho'\rho}(s)BW_\rho(s) + \dots) \quad (35)$$

where  $x_{\rho'\rho}$  is the mixing amplitude which is  $s$ -dependent, in general, and ellipses indicate the mixing of  $\rho'$  with other  $\rho$ -resonances. Suppose one uses a specific dynamical model of  $\rho$  resonances predicting the normalization factors  $c_{\rho,\rho',\dots}$  of the BW-propagators. After including the mixing, the amplitude will have the form (35) with a complicated  $s$ -dependence including an imaginary part. This system of mixed propagators could then be diagonalized, giving in the general case rise to complex couplings between vector mesons and pions. Since we do not attempt to solve this complicated dynamical pattern, in the model of our choice we will keep the coefficients  $c_{\rho,\rho',\dots}$  for few first resonances as free fit parameters and for simplicity, restrict ourselves to real values.

For the description of the infinite series of higher excitations we adopt an ansatz rooted in the Veneziano amplitude and dual resonance models. The specific  $dual-QCD_{N_c=\infty}$  amplitude, suggested in [20], contains an infinite amount of zero-width vector mesons with the quantum numbers of  $\rho$ :

$$F_\pi(s) = \sum_{n=0}^{\infty} c_n \frac{m_n^2}{m_n^2 - s}. \quad (36)$$

For convenience we will count  $\rho$ -resonances by a number  $n$  which starts from  $n = 0$  for the  $\rho$  meson, so that  $\rho'(1450)$  and  $\rho''(1700)$  correspond to  $n = 1, 2$ , respectively. The coefficients

$$c_n = \frac{(-1)^n \Gamma(\beta - 1/2)}{\alpha' \sqrt{\pi} m_n^2 \Gamma(n+1) \Gamma(\beta - 1 - n)} \quad (37)$$

decrease rapidly. The parameter  $\alpha' = 1/(2m_\rho^2)$  is related to the  $\rho$ -meson Regge trajectory:  $\alpha_\rho(s) = 1 + \alpha'(s - m_\rho^2)$ . Furthermore, the model postulates an equidistant mass spectrum:

$$m_n^2 = m_\rho^2(1 + 2n). \quad (38)$$

The parameter  $\beta$  is free and has to be fitted. We will use  $c_0$  fitted from the  $\rho$  region and calculate  $\beta$  from Eq. (37). As we shall see, the fit yields  $c_0 = 1.098 - 1.171$  corresponding to  $\beta = 2.16 \div 2.3$ , in agreement with [20].

Using the above assumptions one easily obtains the form factor in the closed analytical form:

$$F_\pi(s) = \frac{\Gamma(\beta - 1/2)}{\sqrt{\pi} \Gamma(\beta - 1)} B(\beta - 1, 1/2 - \alpha' s), \quad (39)$$

where  $B(x, y)$  is Euler's Beta-function, so that  $F_\pi(0) = 1$ . Importantly, in this model also the mean-squared charge radius of the pion (defined as  $\langle r_\pi^2 \rangle = 6(dF_\pi(s)/ds)|_{s=0}$ ):

$$\langle r_\pi^2 \rangle = 0.42 \div 0.44 \text{ fm}^2, \quad (40)$$

at  $\beta = 2.16 \div 2.3$ , agrees well with the experimental value [30]  $\langle r_\pi^2 \rangle_{exp} = 0.439 \pm 0.008 \text{ fm}^2$  and with the recent chiral perturbation theory determination [31]  $\langle r_\pi^2 \rangle_{ChPT} = 0.452 \pm 0.013 \text{ fm}^2$ .

The most spectacular property of the dual-QCD $_{N_c=\infty}$  model (inherited from Veneziano amplitude) is its explicit duality: in the timelike region the form factor has poles located at  $s = m_n^2$ , whereas in the spacelike region at large  $s < 0$  it exhibits a smooth behaviour with a power-law asymptotic behaviour determined by the parameter  $\beta$ :

$$\lim_{s \rightarrow -\infty} F_\pi(s) \sim \frac{1}{s^{\beta-1}}. \quad (41)$$

With  $\beta = 2.1 - 2.3$  this is very close to the prediction of perturbative QCD.

In [20] the model was further improved by including the constant widths of resonances through the replacement:

$$\frac{m_n^2}{m_n^2 - s - i\epsilon} \rightarrow \frac{m_n^2}{m_n^2 - s - im_n\Gamma_n}. \quad (42)$$

The ansatz [21, 20] adopted for the total widths is again motivated by string-like models:

$$\Gamma_n = \gamma m_n, \quad (43)$$

with  $\gamma = 0.2$  fixed from  $\rho$ . As explained above, to account for the presence of  $2\pi$  and other intermediate multiparticle states coupled to  $\rho$  resonances one has to modify the widths to include  $s$ -dependence with a proper threshold behaviour. Otherwise, the form factor predicts an unphysical imaginary part at  $s = 0$ . Being unable to account for all possible intermediate multiparticle states coupled to each  $\rho_n$  we use, as a remedy, the threshold behaviour of  $\rho_n \rightarrow 2\pi$  partial width attributing it to the total width

$$\Gamma_n(s) = \frac{m_n^2}{s} \left( \frac{p(s)}{p(m_n^2)} \right)^3 \Gamma_n. \quad (44)$$

## 4 The model for the pion form factor

After all these modifications the model [20] for the pion form factor becomes

$$F_\pi(s) = \sum_{n=0}^{\infty} c_n BW_n(s). \quad (45)$$

In its simplest form it depends only on few parameters ( $\beta, \alpha'$  and  $\gamma$ ) and includes infinitely many hadronic degrees of freedom.

Importantly, the coefficients  $c_n$  decrease at  $n \rightarrow \infty$ . Hence starting from  $n \sim 4, 5$ , moderate deviations of  $c_n, m_n, \Gamma_n$  from the model predictions do not influence the form factor, at least in the region of our interest, at  $\sqrt{s} < 2 - 2.5 \text{ GeV}$ . On the other hand, for the most important first four resonances (including  $\rho''' \equiv \rho_3$  with  $m_3 \simeq 2 \text{ GeV}$ ) we

will allow the coefficients, masses and widths to deviate from the dual-QCD $_{N_c=\infty}$  model values, having in mind the effects of coupling to intermediate multiparticle states discussed in the previous section. To large extent, the fitted parameters will be close to those of the dual-QCD $_{N_c=\infty}$  model (see Table 1).

Summarizing, our model for the pion form factor has the following form:

$$F_\pi(s) = \left[ \sum_{n=0}^3 c_n BW_n(s) \right]_{fit} + \left[ \sum_{n=4}^{\infty} c_n BW_n(s) \right]_{dual-QCD_{N_c=\infty}}, \quad (46)$$

where in the  $\rho$  contribution ( $n = 0$ ) the  $\rho - \omega$  mixing is included according to Eq. (33) with the fixed parameters taken from [12]. In the above, the parameters of the four lowest  $\rho_{0,1,2,3}$  states (i.e.  $\rho, \rho'(1450), \rho''(1700)$  and  $\rho'''$ ) are supposed to be fitted to experimental data, whereas the “tail” with the infinite amount of  $\rho_{n>4}$  states is taken as in the dual-QCD $_{N_c=\infty}$  model. However, having in mind the insufficient precision of the current data at  $\sqrt{s} > 1$  GeV, we restrict the number of free fit parameters to the coefficients  $c_{0,1,2}$ , the masses  $m_0$  and  $m_1$  and the total widths  $\Gamma_0$  and  $\Gamma_1$ . The values of  $\Gamma_2$  and  $m_2$  are taken from [26]. The coefficient  $c_3$  of  $\rho_3$  is fixed from the normalization condition for the form factor:

$$c_3 = 1 - (c_0 + c_1 + c_2)_{fit} - \left( \sum_{n=4}^{\infty} c_n \right)_{dual-QCD_{N_c=\infty}}. \quad (47)$$

All remaining parameters in Eq. (46), that is  $c_{n>4}$ ,  $m_{n>3}$ , and  $\Gamma_{n>3}$  are calculated from Eqs. (37), (38) and (44), respectively.

Let us emphasize the main qualitative features of this model. It nicely matches the existing  $\rho$ -dominance models at  $\sqrt{s} < 1$  GeV, such as the ones considered in [12], simply because the  $\rho_{n>2}$  states play a minor role in the  $\sqrt{s} < 1$  GeV region. The model (46) is flexible, that is, it allows to vary the proportion of fitted and modelled resonances above  $\rho$ . E.g., with sufficiently precise data at higher energies one can include also the  $\rho_4$ -state into the ‘fit’ part. Alternatively,  $\rho_3$  can be removed from the ‘fit’ part and added to the dual-QCD $_{N_c=\infty}$  part. Furthermore, as mentioned already,  $F_\pi(s)$ , as given by Eq. (46), can be easily continued to  $s < 0$  and compared with the experimental data and QCD predictions in the spacelike region. Accordingly, one gets a smooth power-like behaviour at asymptotically large timelike  $s$ . Altogether, the model contains a reasonably small amount of free parameters: three per each fitted resonance (the mass, coefficient and total width) and three “global” parameters  $\alpha', \beta, \gamma$ , with  $\alpha' = 1/(2m_\rho^2)$  taken from the Regge trajectory,  $\beta$  taken from Eq. (37) with  $c_0$  derived from the fit, and with  $\gamma = 0.2$ . In principle, one can try to relax and independently fit also the three “global” parameters, but we prefer to keep them fixed. Needless to say, the suggested ansatz has considerable room for improvement, especially concerning the treatment of the effective  $s$ -dependent resonance widths.

We have fitted the model (46) to the existing data [3, 5, 6, 7] for the timelike pion form factor. The results of the fit for the two different versions of BW-formulae: KS (Eq. (30) for all resonances) and GS (Eq. (31) for the first three resonances  $\rho_{0,1,2}$ ), together with the

relevant input parameters are presented in Table 1 and compared with the predictions of the dual-QCD $_{N_c=\infty}$  model. The results for  $|F_\pi(s)|^2$  are plotted in Fig. 1, separately for the

Parameter	Input	Fit(KS)	Fit(GS)	dual-QCD $_{N_c=\infty}$	PDG value [26]
$m_\rho$	-	$773.9 \pm 0.6$	$776.3 \pm 0.6$	input	$775.5 \pm 0.5$
$\Gamma_\rho$	-	$144.9 \pm 1.0$	$150.5 \pm 1.0$	input	$150.3 \pm 1.6$
$m_\omega$	783.0	-	-	-	$782.59 \pm 0.11$
$\Gamma_\omega$	8.4	-	-	-	$8.49 \pm 0.08$
$m_{\rho'}$	-	$1357 \pm 18$	$1380 \pm 18$	1335	$1465 \pm 25$
$\Gamma_{\rho'}$	-	$437 \pm 60$	$340 \pm 53$	266	$400 \pm 60$
$m_{\rho''}$	1700	-	-	1724	$1720 \pm 20$
$\Gamma_{\rho''}$	240	-	-	344	$250 \pm 100$
$m_{\rho'''}^*$	-	-	-	2040	-
$\Gamma_{\rho'''}^*$	-	-	-	400	-
$c_0$	-	$1.171 \pm 0.007$	$1.098 \pm 0.005$	1.171	-
$\beta$	$c_0$ and Eq. (37)	$2.30 \pm 0.01$	$2.16 \pm 0.015$	2.3(input)	-
$c_\omega$	0.00184(KS) 0.00195(GS)	-	-	-	-
$c_1$	-	$-0.119 \pm 0.011$	$-0.069 \pm 0.009$	-0.1171	-
$c_2$	-	$0.0115 \pm 0.0064$	$0.0216 \pm 0.0064$	-0.0246	-
$c_3$	Eq. (47)	$-0.0438 \mp 0.02$	$-0.0309 \mp 0.02$	-0.00995	-
$\sum_{n=4}^{\infty} c_n$	-0.01936	-	-	-0.01936	-
$\chi^2/d.o.f.$	-	155/101	153/101	-	-

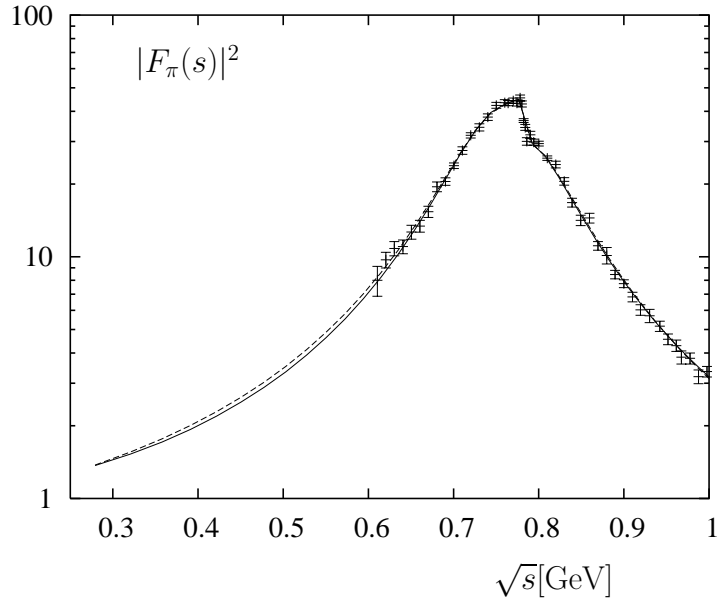
Table 1: Parameters of the pion form factor (46) and results of the fit to the data. Masses and widths are given in MeV. The row 'Fit KS(GS)' contains the fitted values for the case where all  $BW_n$  are taken as in Eq. (30) ( $BW_{0,1,2}$  taken as in Eq. (31)). The sum  $\sum_{n=4}^{\infty} c_n$  is calculated from Eq. (37). The PDG parameters for  $\rho(770)$  are those listed in [26] for "Charged only,  $\tau$  decays and  $e^+e^-$ ". The parameter  $c_\omega$  is taken from [12].

$\sqrt{s} < 1$  GeV and  $\sqrt{s} > 1$  GeV regions.

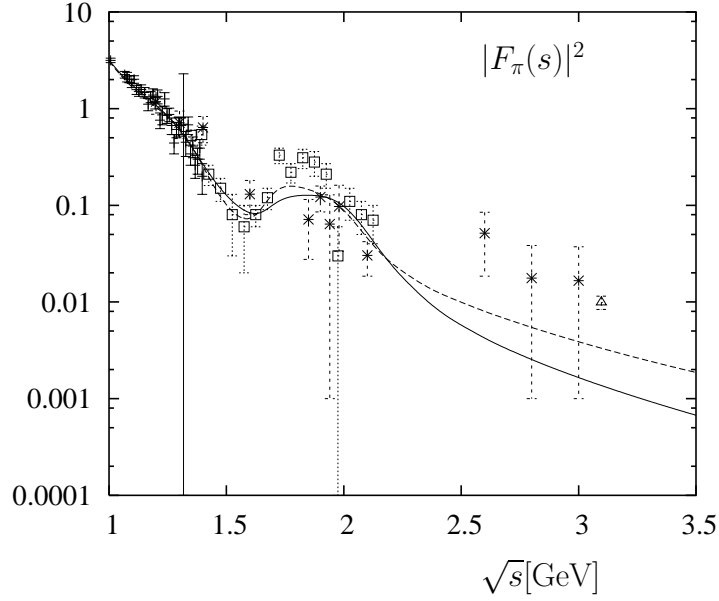
A few comments are in order.

The most spectacular result of the fit is the change of the  $\rho''$  coefficient  $c_2$  with respect to the model [20] and to the earlier fits [12], from negative values  $\sim -(0.02 - 0.04)$  to smaller but positive values  $\sim 0.01-0.02$ . The positive sign is a direct consequence of the dip in the cross section around 1.6 GeV (also the earlier fit of the data in [7] revealed a similar pattern).

Furthermore, the fitted mass of  $\rho'$  gets shifted with respect to the PDG value, the latter obtained by adding together data from all decay channels of  $\rho'$ . Note that a lower  $m_{\rho'}$  consistent with our fit is also obtained by the fits in [12] and predicted by the dual-



(a)



(b)

Figure 1: The pion form factor squared  $|F_\pi(s)|^2$  as a function of  $\sqrt{s}$  fitted to the data in the region near (a) and above (b)  $\rho$  resonance. The solid (dashed) line corresponds to the KS(GS) parameterization of BW formula. Data are taken from [3, 6] (crosses), [5] (stars), and [7] (squares). The triangle point is the value of the form factor extracted from  $J/\psi \rightarrow 2\pi$ .

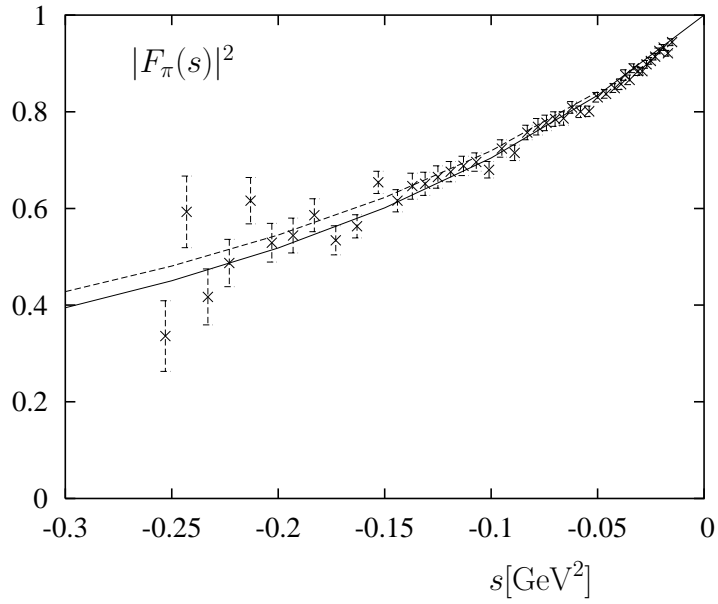
$\text{QCD}_{N_c=\infty}$  model. It is quite probable that a more elaborated model of the total width of  $\rho'$  including multiparticle thresholds will increase the fitted mass. We note that the values of the masses and widths of  $\rho$ ,  $\rho'$ ,  $\rho''$  as well as  $c_0$  and  $c_1$  are in the ballpark of the dual- $\text{QCD}_{N_c=\infty}$  model. The same is true for the magnitude of  $c_2$ , its positive sign is enforced by the dip around 1.6 GeV and might be a consequence of the strong mixing between  $\rho''$  and nearby resonances.

In general, the  $\rho'$ ,  $\rho''$  and  $\rho'''$  terms and their interplay with the contribution of  $\rho$  in both imaginary and real parts of the form factor are the main effects which determine the behavior of  $|F_\pi(s)|^2$  at  $\sqrt{s} > 1$  GeV. In particular, the dip in the form factor observed near  $\sqrt{s} = 1.6$  GeV can only be described by altering the sign of  $c_2$ . The role of the summed “tail” of  $\rho_{n \geq 4}$  states is less important. One has to admit that the quality of the fit is not very high, (we get typically  $\chi^2/\text{d.o.f.} \simeq 1.5$ ), in fact this could simply indicate inconsistencies in the normalization of the various pieces of existing data in the timelike region. Moreover, the data points with large errors at  $\sqrt{s} = 2.5 \div 3$  GeV are systematically higher than the fitted curve, and the value of  $F_\pi(\sqrt{s} = m_{J/\psi})$  extracted from the  $J/\psi \rightarrow 2\pi$  partial width is larger than the model prediction by a factor of about three (this point was not included into the fit). This disagreement deserves a comment. Note that the extraction of  $F_\pi(m_{J/\psi}^2)$  is “theoretically biased”, because one tacitly assumes that the intermediate photon exchange is the only mechanism in this decay. Other mechanisms such as one-photon plus two intermediate gluons could also be important in the  $J/\psi \rightarrow 2\pi$ . Hence, the hadronic matrix element in this isospin-violating transition could be actually different from the pion form factor. Although estimates [29] of gluonic effects based on the perturbative charmonium annihilation are in favour of their smallness, we still think there is room for nonperturbative effects which are however not easily assessed. For the time being it seems difficult to accommodate a pion form factor as large as the one derived from  $J/\psi$  decay. (It will be interesting to check for a similar effect in the  $4\pi$  mode.)

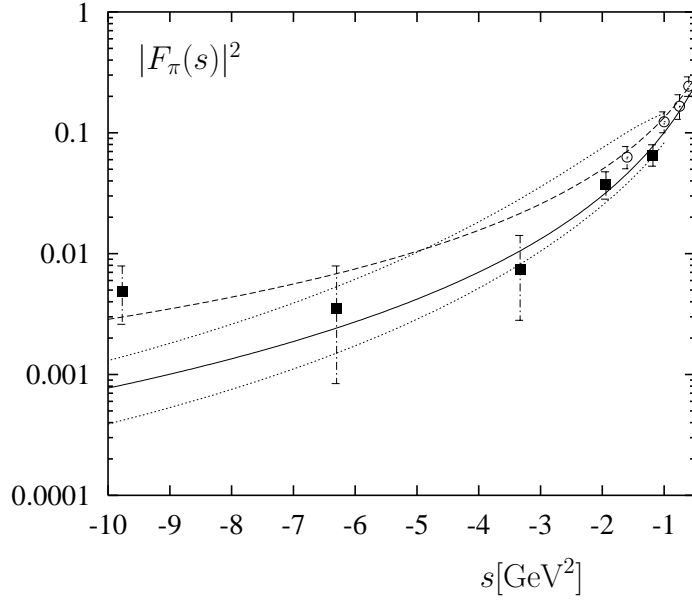
To check our model further we continue  $F_\pi(s)$  to  $s < 0$  and compare the result with the data there (see Fig. 2). The form factor obtained from direct electron-pion scattering at small  $s < 0$  (up to  $|s| = 0.25$  GeV $^2$ ) [30] is not sensitive to the contributions of higher than  $\rho$  resonances, provided the normalization to one at  $s = 0$  is imposed. Note that the fitted form factor (46) predicts  $\langle r_\pi \rangle^2 = 0.440(0.426)$  fm $^2$  for the KS(GS) versions, close to the dual- $\text{QCD}_{N_c=\infty}$  prediction (40) and to the experimental value [30] quoted above.

At larger  $|s|$  the old data [32] obtained from pion electroproduction have large errors and suffer from some intrinsic uncertainties [33]. More accurate data obtained recently at JLab [34] at  $|s| < 1.6$  GeV $^2$  are in agreement with the model, but not sensitive to the details of the fit. Furthermore, there is reasonable agreement between the model and the QCD light-cone sum rule (LCSR) predictions [16, 17]. The latter are taken from [17] with their estimated theoretical uncertainty. The pion form factor calculated from 3-point QCD sum rules [15] in the region of their validity  $|s| \sim 1 \div 4$  GeV $^2$  is within the LCSR interval and therefore not shown separately.

If we try to artificially enhance the form factor at large timelike region, e.g., by enhancing the contribution of the “tail” trying to fit also the point at  $\sqrt{s} = m_{J/\psi}$ , the form factor at spacelike  $s < 0$  increases correspondingly, and the general agreement between



(a)



(b)

Figure 2: The pion form factor squared  $|F_\pi(s)|^2$  as a function of  $s$  in the spacelike region at low  $|s|$  (a) and large  $|s|$  (b). The solid (dashed) line corresponds to the analytic continuation of the timelike form factor (46) with the KS(GS) parameterizations of the BW formula. Data are taken from [30] (crosses), [34] (open circles) and [32] (full squares). Dotted lines at  $|s| > 1 \text{ GeV}^2$  represent the interval derived from QCD light-cone sum rule predictions [17].

data and QCD sum rule predictions is lost. We conclude therefore, just as before, that it is implausible for the form factor obtained on the basis of dual resonance approach to reach values  $|F_\pi(s)|^2 \geq 0.01$  at  $\sqrt{s} = 2.5 \div 3$  GeV without conflicting with the spacelike data and especially with QCD predictions. This statement is independent of many details involved in the timelike form factor model and in the QCD calculations. It is therefore extremely interesting to obtain new accurate data at least up to  $\sqrt{s} = 2.5$  GeV to check this conjecture.

## 5 Charged and neutral kaon e.m. form factors

We now adopt the analogous strategy to describe the kaon form factors. Combining information on  $K^+K^-$  and  $K^0\bar{K}^0$  production with constraints from isospin symmetry, and using assumptions deduced from the quark model and the OZI rule, it is possible to separate the  $I = 1$  and  $I = 0$  amplitudes in the form factor, and even the  $\omega$ - and  $\phi$ -components of the  $I = 0$  part. The  $I = 1$  part can then be used to predict the rate for  $\tau \rightarrow \nu K^- K^0$ .

The electromagnetic form factors for charged and neutral kaons defined similar to Eq. (1):

$$\langle K^+(p_1)K^-(p_2)|j_\mu^{em}|0\rangle = (p_1 - p_2)_\mu F_{K^+}(s) \quad (48)$$

$$\langle K^0(p_1)\bar{K}^0(p_2)|j_\mu^{em}|0\rangle = (p_1 - p_2)_\mu F_{K^0}(s), \quad (49)$$

obey the constraints

$$F_{K^+}(0) = 1, \quad F_{K^0}(0) = 0. \quad (50)$$

They can be separated into their isospin one and zero parts,

$$F_{K^+(K^0)} = F_{K^+(K^0)}^{(I=1)} + F_{K^+(K^0)}^{(I=0)}. \quad (51)$$

From isospin invariance one derives

$$F_{K^+}^{(I=0)} = F_{K^0}^{(I=0)}, \quad F_{K^+}^{(I=1)} = -F_{K^0}^{(I=1)}, \quad (52)$$

and the  $I = 1$  part can furthermore be used to predict the charged current matrix element:

$$\langle K^+(p_1)\bar{K}^0(p_2)|j_\mu^-|0\rangle = (p_1 - p_2)_\mu 2F_{K^+}^{(I=1)}(s). \quad (53)$$

A simultaneous fit to the two electromagnetic form factors leads, therefore, to a direct prediction for the rate for  $\tau \rightarrow \nu K^- K^0$ , without any further assumption.

In the context of vector dominance, combined with the quark model, the kaon form factors are saturated by  $\rho$ ,  $\omega$ ,  $\phi$  and their radial excitations,

$$F_K(s) = \sum_{V=\rho,\omega,\phi,\rho',\omega',\phi',\dots} \frac{\kappa_V f_V g_{VKK} m_V}{m_V^2 - s - im_V \Gamma_V}, \quad (54)$$

and it is the  $\rho$ -mediated  $I = 1$  part which enters both the e.m. and the charged current matrix elements. We define the decay constants of the vector mesons via

$$\langle V|j_\mu^{em}|0\rangle = \kappa_V m_V f_V \epsilon_{(V)}^{\mu*}, \quad (55)$$

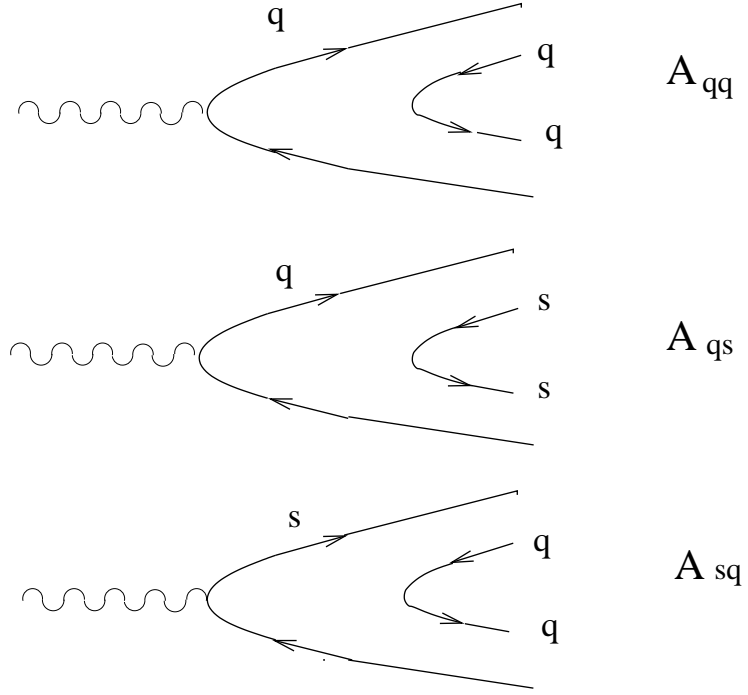


Figure 3: The quark diagrams corresponding to the contributions to the pion and kaon form factors with various flavour combinations.

where  $\epsilon_V$  is the polarization vector of  $V$ , and the coefficients  $\kappa_\rho = 1/\sqrt{2}$  (see Eq. (9)),  $\kappa_\omega = 1/(3\sqrt{2})$  and  $\kappa_\phi = -1/3$  reflect the valence quark content of these mesons corresponding to “ideal” mixing:

$$\rho^0 = \frac{\bar{u}u - \bar{d}d}{\sqrt{2}}, \quad \omega = \frac{\bar{u}u + \bar{d}d}{\sqrt{2}}, \quad \phi = \bar{s}s. \quad (56)$$

The strong coupling is defined as in Eq. (10):

$$\langle K(p_1)\bar{K}(p_2)|V\rangle = (p_2 - p_1)^\nu \epsilon_{\nu(V)} g_{VKK}. \quad (57)$$

In the flavour SU(3)-symmetry limit one evidently has

$$F_{K^+}(s) = F_\pi(s), \quad F_{K^0}(s) = 0. \quad (58)$$

Since this symmetry is broken by the strange-nonstrange quark-mass difference, one has to expect quite noticeable deviations from Eq. (58), in particular the  $K^0$  form factor does not vanish at nonzero  $s$ . Moreover, since  $BR(\phi \rightarrow K^+K^-) \sim BR(\phi \rightarrow K^0\bar{K}^0)$ , the neutral and charged kaon form factors have almost equal magnitudes near the  $\phi$  resonance. In fact, the SU(3)-breaking also manifests itself in the valence quark content of vector mesons given in Eq. (56) and in the mass splitting between  $m_\rho \simeq m_\omega$  and  $m_\phi$ .

In order to derive the kaon form factors in terms of separate vector meson contributions, it is convenient to consider a generic quark diagram of the strong  $VPP$  coupling

and distinguish these diagrams by the presence and position of  $s$  quarks. In the isospin symmetry limit, which we adopt here, there are three different diagrams depicted in Fig. 3: 1) without strange quarks (upper), 2) with  $s$  and  $\bar{s}$  in the  $P\bar{P}$  state only (middle) and 3) with  $s$  and  $\bar{s}$  in the  $V$  and the  $P\bar{P}$  state (bottom). We denote the corresponding hadronic invariant amplitudes  $A_{qq}$ ,  $A_{qs}$  and  $A_{sq}$ . The diagrams with charge conjugated quark lines lead to the same amplitudes with an additional minus sign, taking into account the negative C-parity of neutral vector mesons. The strong couplings of  $\rho, \omega, \phi$  are then expressed in terms of diagrams:

$$\begin{aligned} g_{\rho^0\pi^+\pi^-} &\equiv g_{\rho\pi\pi} = \sqrt{2}A_{qq}, \\ g_{\rho^0K^+K^-} &= g_{\omega K^+K^-} = \frac{1}{\sqrt{2}}A_{qs}, \quad g_{\rho^0K^0\bar{K}^0} = -g_{\omega K^0\bar{K}^0} = -\frac{1}{\sqrt{2}}A_{qs}, \\ g_{\phi K^+K^-} &= g_{\phi K^0\bar{K}^0} = -A_{sq}. \end{aligned} \quad (59)$$

Thus, from the quark model one expects approximately equal  $K\bar{K}\rho$  and  $K\bar{K}\omega$  couplings. It is easy to check that this simple formalism correctly reproduces  $g_{\omega\pi^+\pi^-} = g_{\rho\pi^0\pi^0} = 0$ , as well as SU(3)-symmetry relations between the couplings. In what follows we also use the relation between the decay constants of  $\omega$  and  $\rho$  following from Eq. (55):  $f_\omega = f_\rho$ . Substituting the decay constants and hadronic couplings (59) to Eq. (54) we obtain the desired decompositions of the kaon form factors in terms of vector meson contributions:

$$F_{K^+}(s) = \frac{f_\rho A_{qs}}{2m_\rho} BW_\rho(s) + \frac{f_\rho A_{qs}}{6m_\omega} BW_\omega(s) + \frac{f_\phi A_{sq}}{3m_\phi} BW_\phi(s), \quad (60)$$

$$F_{K^0}(s) = -\frac{f_\rho A_{qs}}{2m_\rho} BW_\rho(s) + \frac{f_\rho A_{qs}}{6m_\omega} BW_\omega(s) + \frac{f_\phi A_{sq}}{3m_\phi} BW_\phi(s). \quad (61)$$

Written in the same terms the pion form factor is

$$F_\pi(s) = \frac{f_\rho A_{qq}}{m_\rho} BW_\rho(s), \quad (62)$$

and  $f_\rho A_{qq}/m_\rho = 1$  in the simplest version of VDM. In the SU(3) limit  $f_\rho = f_\phi$ ,  $m_\rho = m_\omega = m_\phi$ ,  $A_{qq} = A_{qs} = A_{sq}$  and the relations (58) are reproduced. In Eqs. (60) and (61) we will adopt the KS version of BW formulae for  $\rho$ , and the analogous  $s$ -dependent width for  $\phi$ ,

$$\Gamma_\phi(s) = \frac{m_\phi^2}{s} \left( \frac{p^K(s)}{p^K(m_\phi^2)} \right)^3 \Gamma_\phi. \quad (63)$$

with  $\Gamma_\phi \equiv \Gamma^{tot}(\phi)$  and  $p^K(s) = (s - 4m_K^2)^{1/2}/2$ . For simplicity, we assume that the effective threshold of all  $\phi$  decay modes including  $\phi \rightarrow 3\pi$  is approximated by Eq. (63), having in mind that the non- $KK$  channels give only about 20% of  $\Gamma_\phi$ . Naturally, the possibility to use the GS-form in Eqs. (60) and (61) exists, yielding inessential differences. For simplicity, to avoid complicated  $3\pi$ -threshold factors we will use constant widths for  $\omega$ , having in mind

that the thresholds are much lower than the boundary of the physical region of the form factor:  $9m_\pi^2 \ll 4m_K^2$ . This is a good approximation at least for the narrow  $\omega$  resonance.

Adding radial excitations to all ground-state vector mesons is the next natural step. From the pion form factor analysis we already learned that the ‘‘tails’’ of higher resonances are numerically inessential. For the kaon form factor we therefore restrict the analysis to the excited states  $\rho'$ ,  $\rho''$ ,  $\omega' \equiv \omega(1420)$ ,  $\omega'' \equiv \omega(1650)$  and  $\phi' \equiv \phi(1680)$  [26]. Higher excitations, as well as more elaborated  $s$ -dependent widths, can be installed in the future when more accurate data will be available. Since the products of decay constants and strong couplings in Eqs. (60) and (61) will not be separated and have to be fitted as a whole, it is convenient to introduce again the normalization factors  $c_V^K$  instead of these products. The ansatz for the kaon form factors thus reads:

$$\begin{aligned} F_{K^+}(s) = & \frac{1}{2}(c_\rho^K BW_\rho(s) + c_{\rho'}^K BW_{\rho'}(s) + c_{\rho''}^K BW_{\rho''}(s)) \\ & + \frac{1}{6}(c_\omega^K BW_\omega(s) + c_{\omega'}^K BW_{\omega'}(s) + c_{\omega''}^K BW_{\omega''}(s)) \\ & + \frac{1}{3}(c_\phi BW_\phi(s) + c_{\phi'} BW_{\phi'}(s)), \end{aligned} \quad (64)$$

$$\begin{aligned} F_{K^0}(s) = & -\frac{1}{2}(c_\rho^K BW_\rho(s) + c_{\rho'}^K BW_{\rho'}(s) + c_{\rho''}^K BW_{\rho''}(s)) \\ & + \frac{1}{6}(c_\omega^K BW_\omega(s) + c_{\omega'}^K BW_{\omega'}(s) + c_{\omega''}^K BW_{\omega''}(s)) \\ & + \frac{1}{3}(\eta_\phi c_\phi BW_\phi(s) + c_{\phi'} BW_{\phi'}(s)), \end{aligned} \quad (65)$$

The widths are with  $p$ -wave factors for  $\rho$  and  $\phi$  states as explained above, and constant for  $\omega$ -states, which is however a rather crude approximation for  $\omega'$ ,  $\omega''$ . The ansatz in Eqs. (64) and (65) reflects isospin invariance and the hierarchy of vector meson contributions according to their valence-quark content, however, it allows for the possibility of SU(3) violations which could and will manifest in differences between the fitted normalization coefficients. The additional factor  $\eta_\phi$  in Eq. (65) takes into account the isospin-breaking difference between the charged and neutral kaon couplings to  $\phi$ :

$$\eta_\phi \equiv \frac{g_{\phi K^0 \bar{K}^0}}{g_{\phi K^+ K^-}} = \left( \frac{BR(\phi \rightarrow K^0 \bar{K}^0)(m_\phi^2 - 4m_{K^+}^2)^{3/2}}{BR(\phi \rightarrow K^+ K^-)(m_\phi^2 - 4m_{K^0}^2)^{3/2}} \right)^{1/2}. \quad (66)$$

According to [26] the central value of this factor slightly deviates from the unit:

$$\eta_\phi = 1.027 \pm 0.01. \quad (67)$$

In the vicinity of the  $\phi$  resonance this small effect is noticeable in the fit, and as far as the branching ratio is concerned, is dominated by the phase space factor. The factor  $\eta_\phi$  also takes care of Coulomb-rescattering and other isospin-violating differences between charged

and neutral modes (see also [35, 36]). To ensure the proper normalizations  $F_{K^0}(0) = 0$  and  $F_{K^+}(0) = 1$ , we introduce an additional energy dependence with a simple step-function

$$\eta_\phi(s) = 1 + (\eta_\phi - 1)\theta(\sqrt{s} - (m_\phi - \Gamma_\phi))\theta(m_\phi + \Gamma_\phi - \sqrt{s}), \quad (68)$$

which in future, after this effect is better understood both experimentally and theoretically, can be replaced by an appropriate analytical energy-dependence.

We have fitted the model (64) and (65) to the available data on charged [37, 38, 39, 40, 41] and neutral [4, 37, 42, 43] kaon form factors. The masses and widths of  $\rho$ ,  $\omega$  and their excitations are taken from [26] and are listed in the Table 2. Two different variants of the fit are carried out:

(1) the *constrained* fit (motivated by the quark model) where the normalization factors for  $\omega$  resonances are fixed:  $c_{\omega,\omega',\omega''}^K = c_{\rho,\rho',\rho''}^K$  and only the normalization factors for the  $\rho$  resonances are fitted;

(2) the *unconstrained* fit, where  $\omega$ - and  $\rho$ - factors are fitted as independent parameters.

First, the mass and width of  $\phi$  as well as the coefficient  $\eta_\phi$  are fitted in the region around  $\phi$  resonance. We obtain:  $\eta_\phi = 1.011 \pm 0.009$  ( $1.019 \pm 0.009$ ) for the constrained (unconstrained) fit, in a good agreement with the experimental value (67). Fixing  $\eta_\phi$  and using  $m_\phi$  and  $\Gamma_\phi$  as starting values, the data in the whole region of  $\sqrt{s}$  are then fitted. The results of the fit are collected in Table 2. The best (i.e., stable and physically plausible) results for both variants of the fit are obtained if data on  $F_{K^+}$  and  $F_{K^0}$  are fitted simultaneously. Thus, predicting  $F_{K^0}$  from  $F_{K^+}$  with the currently available data is not yet possible. The resulting curves for the form factors are plotted in Figs. 4,5. Most importantly, fitting the kaon form factor above  $\phi$  resonance, it is indeed possible to extract separate  $\rho$ ,  $\omega$ ,  $\phi$  components, which was not possible in the  $\phi$  region due to the dominance of this resonance.

We also find the pattern of the normalization factors  $c_{\rho,\rho'}^K$  for the first two  $\rho$ -resonance to be very similar to the corresponding values  $c_{0,1}$  obtained in the pion form factor fits. These factors can be immediately translated into the strong couplings dividing out the decay constants of vector mesons. The latter are independently measured in the leptonic decays revealing a very mild SU(3) breaking, at the level of 10 %; according to the data in [26]:  $f_\rho \simeq 220$  MeV,  $f_\omega \simeq 195$  MeV and  $f_\phi \simeq 228$  MeV. The SU(3)-violating difference between the couplings of  $\rho$  and  $\phi$  to kaons estimated from comparing  $c_\rho^K$  and  $c_\phi^K$  is also moderate in both versions of the fit.

As already noticed above, the constraint  $c_\omega^K = c_\rho^K$  naturally follows from the valence quark content of both mesons and we consider this constraint as a part of our model. The fact that the unconstrained fit gives about 25% difference between these two coefficients, a noticeable deviation from the quark-diagram relation, should be taken with caution, having in mind poor quality of data. Also  $\chi^2$ 's of both fits are in the same ballpark, so that from the fitting point of view we cannot yet give any preference to the version with the “floating” couplings of  $\omega$ -resonances. On the other hand, this difference indicates that the fit is able to resolve also the “fine structure” of the couplings. The differences between the normalization factors given by the fit for excited resonances:  $c_\rho^K$  vs.  $c_{\omega'}^K$  (in the

Parameter	Input	Fit(1)	Fit(2)	PDG value[26]
$m_\phi$	-	$1019.372 \pm 0.02$	$1019.355 \pm 0.02$	$1019.456 \pm 0.02$
$\Gamma_\phi$	-	$4.36 \pm 0.05$	$4.29 \pm 0.05$	$4.26 \pm 0.05$
$m_{\phi'}$	1680	-	-	$1680 \pm 20$
$\Gamma_{\phi'}$	150	-	-	$150 \pm 50$
$m_\rho$	775	-	-	$775.8 \pm 0.5$
$\Gamma_\rho$	150	-	-	$150.3 \pm 1.6$
$m_{\rho'}$	1465	-	-	$1465 \pm 25$
$\Gamma_{\rho'}$	400	-	-	$400 \pm 60$
$m_{\rho''}$	1720	-	-	$1720 \pm 20$
$\Gamma_{\rho''}$	250	-	-	$250 \pm 100$
$m_\omega$	783.0	-	-	$782.59 \pm 0.11$
$\Gamma_\omega$	8.4	-	-	$8.49 \pm 0.08$
$m_{\omega'}$	1425	-	-	1400-1450
$\Gamma_{\omega'}$	215	-	-	180-250
$m_{\omega''}$	1670	-	-	$1670 \pm 30$
$\Gamma_{\omega''}$	315	-	-	$315 \pm 35$
$c_\phi$	-	$1.018 \pm 0.006$	$0.999 \pm 0.007$	-
$c_{\phi'}$	$1 - c_\phi^K$	$-0.018 \mp 0.006$	$0.001 \mp 0.007$	-
$c_\rho^K$	-	$1.195 \pm 0.009$	$1.139 \pm 0.010$	-
$c_{\rho'}^K$	-	$-0.112 \pm 0.010$	$-0.124 \pm 0.012$	-
$c_{\rho''}^K$	$1 - c_\rho^K - c_{\rho'}^K$	$-0.083 \mp 0.019$	$-0.015 \mp 0.022$	-
$c_\omega^K(1)$	$c_\rho^K$	$1.195 \pm 0.009$	-	-
$c_\omega^K(2)$	-	-	$1.467 \pm 0.035$	-
$c_{\omega'}^K(1)$	$c_{\rho'}^K$	$-0.112 \pm 0.010$	-	-
$c_{\omega'}^K(2)$	-	-	$-0.018 \pm 0.024$	-
$c_{\omega''}^K$	$1 - c_\omega^K - c_{\omega'}^K$	$-0.083 \mp 0.019$	$-0.449 \mp 0.059$	-
$\chi^2/d.o.f.$	-	328/242	281/240	-

Table 2: *Parameters of the kaon form factors and results of the fit to the data. Masses and widths are given in MeV. The row 'Fit(1)' (Fit(2)) contains the values of the constrained (unconstrained) fits.*

unconstrained fit),  $c_{\rho'}^K$  vs.  $c_{\phi'}$ , etc. are generally large, which is not surprising, in view of the complicated mixing between all these states. Including in the future more precise data and switching on the “tails” of the dual QCD $_{N_c=\infty}$  amplitudes in the kaon form factors for all three vector mesons will allow to reveal these differences more accurately.

Furthermore, an indication for an excess of the measured charged kaon form factor vs. the model is present in Fig. 4b in the region around 2 GeV, although the experimental errors are large. Remember, that we have not included in our fit the contribution of the second excited  $\phi''$  state with a mass around 2 GeV, which might be responsible for this potential difference. However, we refrain from further investigation before more accurate data are available.

The mean-squared charge radius of the  $K^+$  obtained in our model:  $\sqrt{\langle r_K^2 \rangle} = 0.56$  fm (for both fits and with a small error), is in a good agreement with the experimental value [44]  $\sqrt{\langle r_K^2 \rangle}_{exp} = 0.53 \pm 0.05$  fm. We have also checked that, being analytically continued to large  $s < -1\text{GeV}^2$ , the charged kaon form factor agrees with the LCSR prediction obtained in [17].

Finally, as mentioned in the Introduction, the separate reconstruction of  $I = 0$  and  $I = 1$  spectral functions might be a useful ingredient for various phenomenological analyses. In Fig. 6 we display the spectral functions defined as

$$\rho_{K\bar{K}}^{(I=0,1)}(s) = \frac{1}{12\pi} \left| \frac{F_{K^+}(s) \pm F_{K^0}(s)}{2} \right|^2 \left( \frac{2p_K(s)}{\sqrt{s}} \right)^3, \quad (69)$$

noticing that this observable is quite sensitive to the pattern of resonances in the form factor.

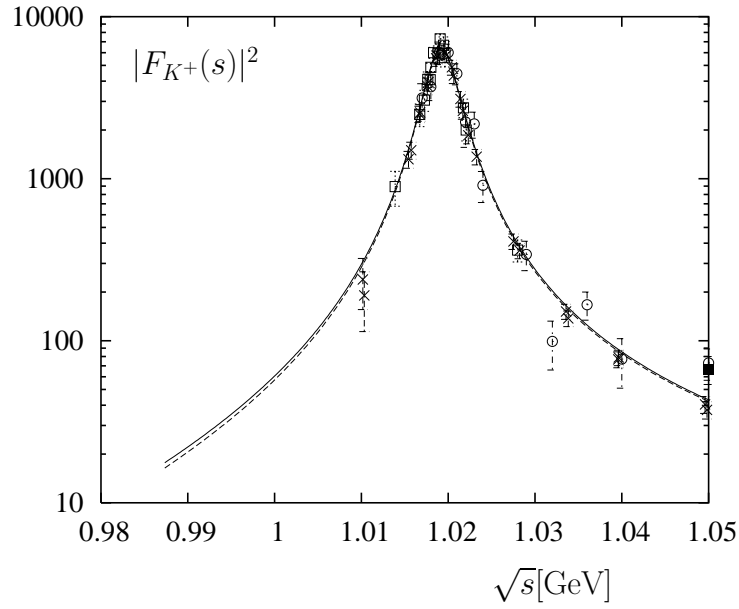
## 6 Predicting $\tau \rightarrow K^- K^0 \nu_\tau$ decay distribution and rate

As emphasized above, the isospin one part of the e.m. kaon form factor, together with the isospin-symmetry relation (53), can be used to predict the  $\tau \rightarrow K^- K^0 \nu_\tau$  decay width. The differential decay distribution in  $\sqrt{Q^2}$  (the invariant mass of the kaon pair), normalized to the leptonic width of  $\tau$  reads:

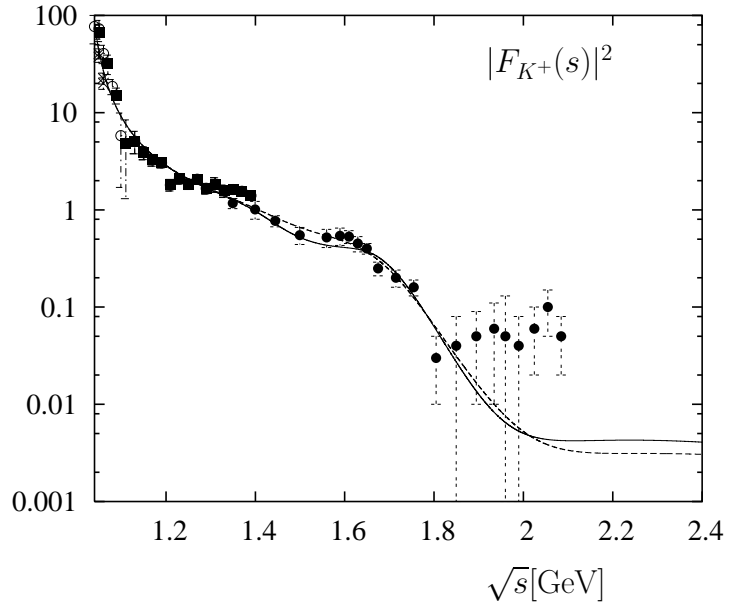
$$\begin{aligned} & \left( \frac{1}{BR(\tau \rightarrow \mu^- \bar{\nu}_\mu \nu_\tau)} \right) \frac{dBR(\tau \rightarrow K^- K^0 \nu_\tau)}{d\sqrt{Q^2}} \\ &= \frac{|V_{ud}|^2}{2m_\tau^2} \left( 1 + \frac{2Q^2}{m_\tau^2} \right) \left( 1 - \frac{Q^2}{m_\tau^2} \right)^2 \left( 1 - \frac{4m_K^2}{Q^2} \right)^{3/2} \sqrt{Q^2} |F_{K^- K^0}(Q^2)|^2. \end{aligned} \quad (70)$$

In accordance with the isospin limit, we neglect the mass difference between charged and neutral kaons and the effect of the scalar form factor. Using Eq. (53) we have  $F_{K^- K^0} = -2F_{K^+}^{(I=1)}$ , hence

$$|F_{K^- K^0}(Q^2)|^2 = |c_\rho^K BW_\rho(Q^2) + c_{\rho'}^K BW_{\rho'}(Q^2) + c_{\rho''}^K BW_{\rho''}(Q^2)|^2. \quad (71)$$

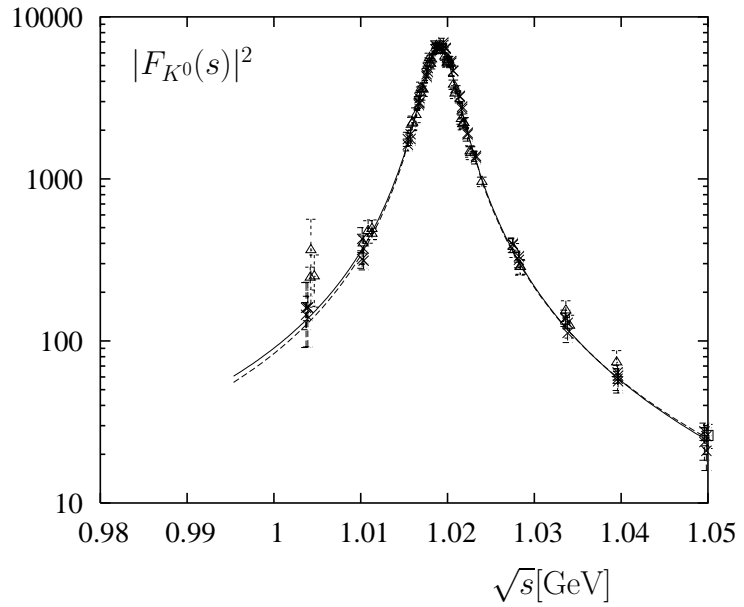


(a)

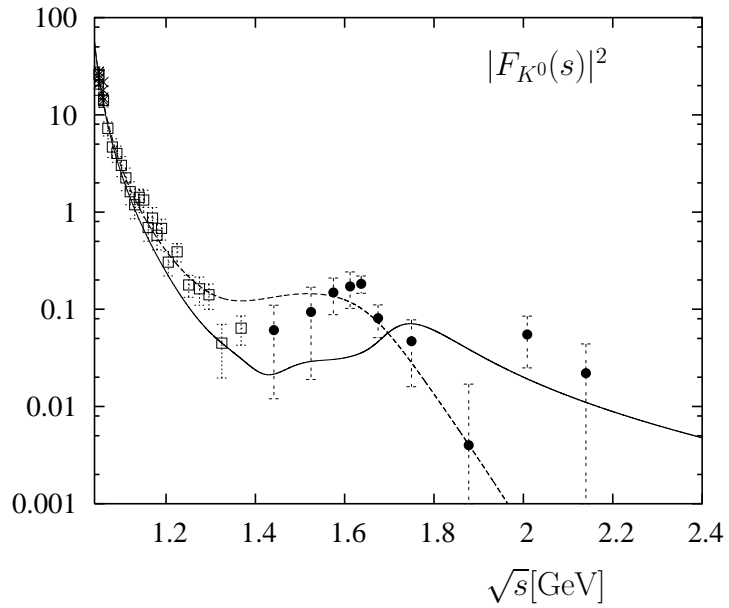


(b)

Figure 4: The charged kaon form factor squared  $|F_{K^+}(s)|^2$  as a function of  $\sqrt{s}$  fitted to the data taken from [37] (crosses), [38] (open squares), [39] (open circles), [40] (full squares) and [41] (full circles). The solid(dashed) lines correspond to the constrained (unconstrained) fit.

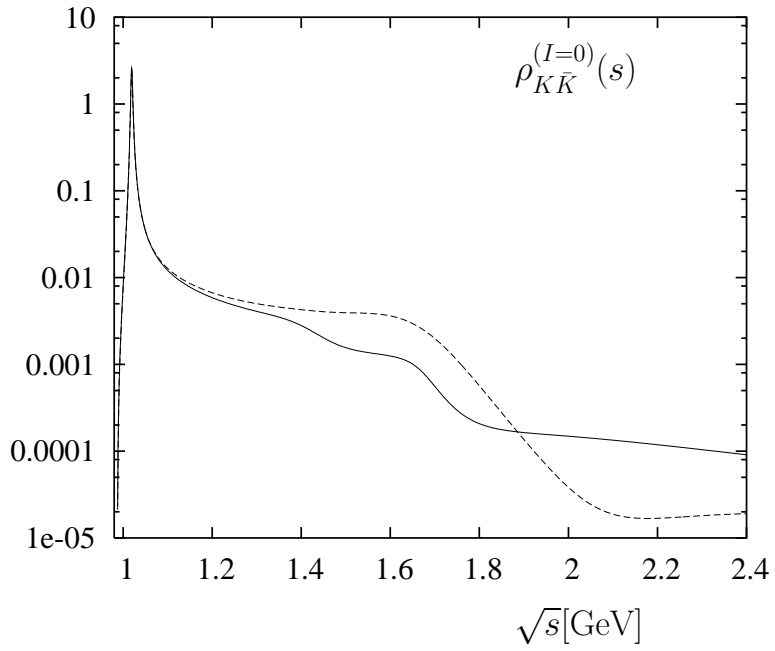


(a)

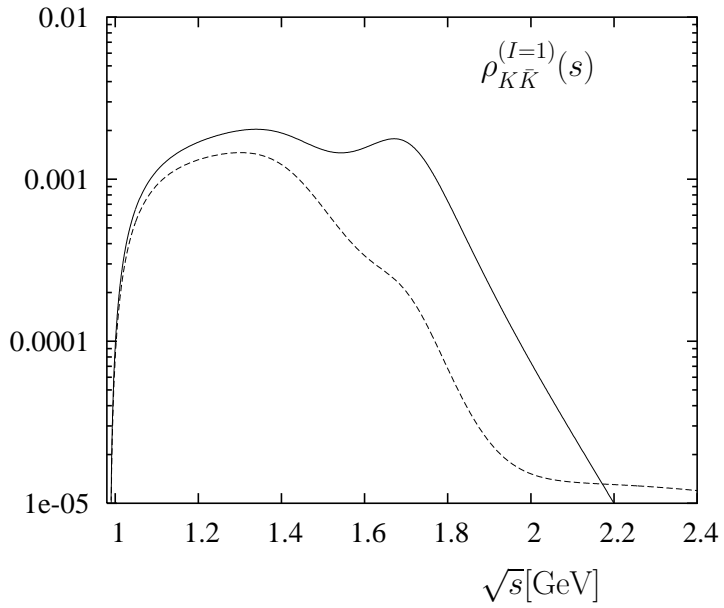


(b)

Figure 5: The neutral kaon form factor squared  $|F_{K^0}(s)|^2$  as a function of  $\sqrt{s}$  fitted to the data taken from [4](triangles), [37](crosses), [42](open squares) and [43](full circles). The solid(dashed) lines correspond to the constrained (unconstrained) fit.



(a)



(b)

Figure 6: The spectral functions (69) with  $I = 0$  (a) and  $I = 1$  (b) obtained from the fitted kaon form factors. The solid(dashed) lines correspond to the constrained (unconstrained) fit.

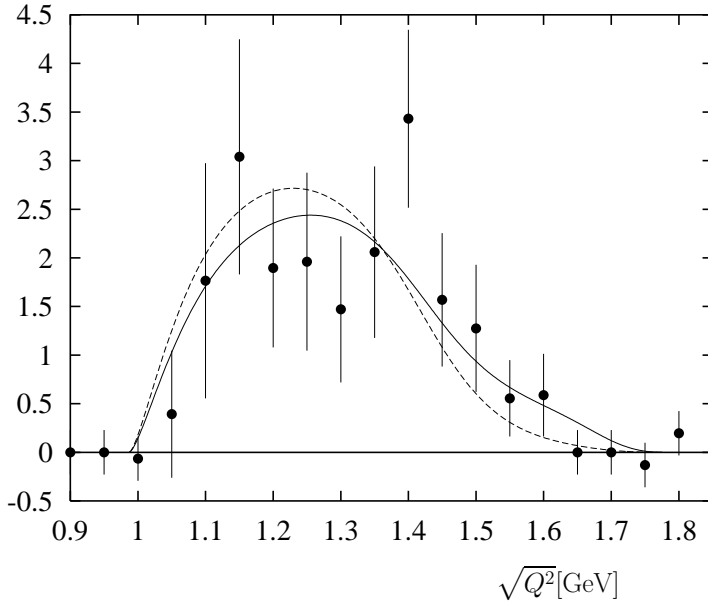


Figure 7: The normalized distribution  $\frac{d\Gamma(\tau \rightarrow K^- K^0 \nu_\tau)}{\Gamma(\tau \rightarrow K^- K^0 \nu_\tau)} / d\sqrt{Q^2}$  in the kaon pair invariant mass  $\sqrt{Q^2}$  in units of  $\text{GeV}^{-1}$  obtained from the fitted kaon form factor; the solid (dashed) line corresponds to the constrained (unconstrained) fit. The event distribution measured by CLEO Collaboration [45] and normalized, dividing by the total number of events, is shown with points.

The fitted values for  $c_{\rho, \rho', \rho''}^K$  from Table 2 thus allow us to calculate the decay distribution (70). The normalized distribution is plotted in Fig. 7 and (qualitatively) compared with the event distribution in the kaon pair mass, measured by CLEO Collaboration [45]. Another measurement of this distribution by ALEPH Collaboration can be found in [46]. Integrating over  $\sqrt{Q^2}$  from  $2m_K$  to  $m_\tau$  we obtain the branching ratio

$$BR(\tau \rightarrow K^- K^0 \nu_\tau) = 0.19 \pm 0.01\% \quad (0.13 \pm 0.01\%) \quad (72)$$

for the constrained (unconstrained) fit, to be compared with the experimentally measured value [26]

$$BR(\tau \rightarrow K^- K^0 \nu_\tau) = 0.154 \pm 0.016\%. \quad (73)$$

We see that both the decay distribution and the decay width are very sensitive to the pattern of  $\rho$  resonances in the isospin-1 form factor. Generally, the width grows with the increase of the excited  $\rho$  contributions, an effect observed earlier in [47] (see also [48]).

## 7 Conclusions

In this paper we considered the models of timelike form factors of pions and kaons in anticipation of new and more accurate data in the region above 1 GeV, from  $e^+e^-$  machines using the radiative return method. We introduced an ansatz for the pion form factor which is based on dual-resonance models and Veneziano amplitude. We argued that the parameters of the ground-state and first excited states can deviate from the model prediction due to effects of mixing with multiparticle (e.g., two - or 4  $\pi$  states), therefore have to be fitted independently as free parameters. From the fit to the available pion form factor data we have found that the main contribution to the form factor originates from the ground state plus the first two-three radially excited states. The tail from the infinite series of resonances produces inessential, but visible effects. The sign and value of the coefficients at certain excited resonances are shifted with respect to the dual  $QCD_{N_c=\infty}$  ansatz signaling large mixing effects. Possible checks of the model are provided by the spacelike form factors, the pion charge radius and the behaviour for large  $s$  in the timelike region. In particular around  $\sqrt{s} = 3$  GeV we predict a value smaller than the one anticipated from  $J/\psi$  decay. On the other hand, data fitted to this model can be used for important tests of quark-hadron duality, and of the QCD calculations of the pion form factor in the spacelike region.

Furthermore, we formulated an analogous model for the kaon form factor and demonstrated that the contributions of  $\phi$ ,  $\omega$  and  $\rho$  resonances (or, alternatively, the isospin 0 and 1 components) can be separated by the fit. Interestingly, the  $\tau \rightarrow K^- K^0 \nu_\tau$ -decay distribution and partial width predicted from the model manifest a substantial sensitivity to the pattern of  $\rho$  resonances in the isospin-1 part of the form factor.

The model still has considerable room for improvement. In particular, a more detailed kinematical and dynamical analysis of total widths in the Breit-Wigner factors would allow to implement a more accurate energy-dependence in these widths.

### Acknowledgements

We are grateful to S. Eidelman for a useful discussion. This work is supported by the German Ministry for Education and Research (BMBF).

## References

- [1] M. Davier, S. Eidelman, A. Hocker and Z. Zhang, Eur. Phys. J. C **31** (2003) 503; hep-ph/0308213(v2).
- [2] K. Hagiwara, A. D. Martin, D. Nomura and T. Teubner, Phys. Rev. D **69** (2004) 093003.
- [3] R. R. Akhmetshin *et al.* [CMD-2 Collaboration], Phys. Lett. B **527** (2002) 161.
- [4] R. R. Akhmetshin *et al.* [CMD-2 Collaboration], Phys. Lett. B **578** (2004) 285.

- [5] D. Bollini, P. Giusti, T. Massam, L. Monari, F. Palmonari, G. Valenti and A. Zichichi, Lett. Nuovo Cim. **14** (1975) 418.
- [6] L. M. Barkov *et al.*, Nucl. Phys. B **256**, 365 (1985).
- [7] D. Bisello *et al.* [DM2 Collaboration], Phys. Lett. B **220** (1989) 321.
- [8] S. Binner, J. H. Kuhn and K. Melnikov, Phys. Lett. B **459** (1999) 279.
- [9] A. Aloisio *et al.* [KLOE Collaboration], arXiv:hep-ex/0407048.
- [10] E. P. Solodov [BABAR collaboration], in *Proc. of the  $e^+e^-$  Physics at Intermediate Energies Conference* ed. Diego Bettoni, eConf **C010430** (2001) T03 [arXiv:hep-ex/0107027].
- [11] B. V. Geshkenbein and M. V. Terentev, Sov. J. Nucl. Phys. **40**, 487 (1984).
- [12] J. H. Kühn and A. Santamaria, Z. Phys. C **48** (1990) 445.
- [13] G. P. Lepage and S. J. Brodsky, Phys. Lett. **87B** (1979) 359; Phys. Rev. **D22** (1980) 2157;  
A. V. Efremov and A. V. Radyushkin, Phys. Lett. **B94** (1980) 245; Theor. Math. Phys. **42** (1980) 97;  
V. L. Chernyak and A. R. Zhitnitsky, JETP Lett. **25** (1977) 510; Sov. J. Nucl. Phys. **31** (1980) 544;  
G. R. Farrar and D. R. Jackson, Phys. Rev. Lett. **43** (1979) 246.
- [14] N. Isgur and C. H. Llewellyn Smith, Phys. Lett. B **217**, 535 (1989);  
A. V. Radyushkin, Nucl. Phys. A **527**, 153C (1991); A **532**, 141 (1991);  
R. Jakob and P. Kroll, Phys. Lett. B **315**, 463 (1993) [Erratum-ibid. B **319**, 545 (1993)].
- [15] B. L. Ioffe and A. V. Smilga, Nucl. Phys. B **216**, 373 (1983);  
V. A. Nesterenko and A. V. Radyushkin, Phys. Lett. B **115**, 410 (1982);  
V. V. Braguta and A. I. Onishchenko, Phys. Lett. B **591** (2004) 267.
- [16] V. M. Braun and I. E. Halperin, Phys. Lett. B **328**, 457 (1994);  
V. M. Braun, A. Khodjamirian and M. Maul, Phys. Rev. D **61**, 073004 (2000).
- [17] J. Bijnens and A. Khodjamirian, Eur. Phys. J. C **26** (2002) 67.
- [18] T. Gousset and B. Pire, Phys. Rev. D **51** (1995) 15.
- [19] A. P. Bakulev, A. V. Radyushkin and N. G. Stefanis, Phys. Rev. D **62** (2000) 113001.
- [20] C. A. Dominguez, Phys. Lett. B **512** (2001) 331.

- [21] P. H. Frampton, Phys. Rev. D **1**, 3141 (1970);  
 N. Tokuda and Y. Oyanagi, Phys. Rev. D **1**, 2626 (1970);  
 L. F. Urrutia, Phys. Rev. D **9**, 3213 (1974);  
 R. Jengo and E. Remiddi, Nuovo Cimento Lett. **18**, 922 (1969).
- [22] M. A. Shifman, in 'At the Frontier of Particle Physics/Handbook of QCD', ed. M. Shifman (World Scientific, Singapore, 2001). arXiv:hep-ph/0009131;  
 B. V. Geshkenbein and V. L. Morganov, arXiv:hep-ph/9410252;  
 M. V. Polyakov and V. V. Vereshagin, Phys. Rev. D **54**, 1112 (1996);  
 S. Peris, B. Phily and E. de Rafael, Phys. Rev. Lett. **86**, 14 (2001);  
 S. S. Afonin, A. A. Andrianov, V. A. Andrianov and D. Espriu, arXiv:hep-ph/0403268.
- [23] F. Jegerlehner, Z. Phys. C **32**, 195 (1986).
- [24] H. Leutwyler, in Continuous advances in QCD 2002, pp.23-40, World Scientific (2002), arXiv:hep-ph/0212324.
- [25] G. J. Gounaris and J. J. Sakurai, Phys. Rev. Lett. **21** (1968) 244.
- [26] S. Eidelman *et al.* [Particle Data Group Collaboration], Phys. Lett. B **592** (2004) 1. (see also <http://pdg.lbl.gov/2004/listings/>)
- [27] H. Czyz and J. H. Kuhn, Eur. Phys. J. C **18**, 497 (2001.)
- [28] N. N. Achasov and A. A. Kozhevnikov, Phys. Rev. D **55** (1997) 2663.
- [29] J. Milana, S. Nussinov and M. G. Olsson, Phys. Rev. Lett. **71**, 2533 (1993).
- [30] S. R. Amendolia *et al.* [NA7 Collaboration], Nucl. Phys. B **277** (1986) 168.
- [31] J. Bijnens and P. Talavera, JHEP **0203** (2002) 046.
- [32] C. J. Bebek *et al.*, Phys. Rev. D **17** (1978) 1693.
- [33] C. E. Carlson and J. Milana, Phys. Rev. Lett. **65**, 1717 (1990).
- [34] J. Volmer *et al.* [The Jefferson Lab F(pi) Collaboration], Phys. Rev. Lett. **86**, 1713 (2001).
- [35] M. B. Voloshin, arXiv:hep-ph/0402171.
- [36] A. Bramon, R. Escribano, J. L. Lucio M. and G. Pancheri, Phys. Lett. B **486** (2000) 406.
- [37] M. N. Achasov *et al.*, Phys. Rev. D **63**, 072002 (2001).
- [38] R. R. Akhmetshin *et al.*, Phys. Lett. B **364**, 199 (1995).
- [39] P. M. Ivanov *et al.*, Phys. Lett. B **107**, 297 (1981).

- [40] S. I. Dolinsky *et al.*, Phys. Rept. **202**, 99 (1991).
- [41] D. Bisello *et al.* [DM2 Collaboration], Z. Phys. C **39**, 13 (1988).
- [42] R. R. Akhmetshin *et al.*, Phys. Lett. B **551** (2003) 27.
- [43] F. Mane, D. Bisello, J. C. Bizot, J. Buon, A. Cordier and B. Delcourt, Phys. Lett. B **99**, 261 (1981).
- [44] E. B. Dally *et al.*, Phys. Rev. Lett. **45** (1980) 232.
- [45] T. E. Coan *et al.* [CLEO Collaboration], Phys. Rev. D **53** (1996) 6037.
- [46] R. Barate *et al.* [ALEPH Collaboration], Eur. Phys. J. C **4** (1998) 29.
- [47] M. Finkemeier, J. H. Kühn and E. Mirkes, Nucl. Phys. Proc. Suppl. **55C**, 169 (1997).
- [48] S. I. Eidelman and V. N. Ivanchenko, Phys. Lett. B **257** (1991) 437.